Available online at www.sciencedirect.com
SCIENCE DIRECT®
Thermochimica Acta 412 (2004) 163–170
thermochimica acta
www.elsevier.com/locate/tca

Solid–liquid phase diagrams of binary salt hydrate mixtures involving magnesium nitrate and acetate, magnesium and aluminum nitrates, ammonium alum and sulfate, and ammonium alum and aluminum sulfate

Y. Marcus*, A. Minevich, L. Ben-Dor

Department of Inorganic and Analytical Chemistry, The Hebrew University, Jerusalem 91904, Israel

Received 3 June 2003; received in revised form 24 September 2003; accepted 24 September 2003

Abstract

The solid–liquid phase diagrams of binary mixtures of magnesium nitrate hexahydrate with magnesium acetate tetrahydrate and with aluminum nitrate nonahydrate and of ammonium alum with ammonium sulfate and with aluminum sulfate octa- or hexadecahydrate are presented. The phase diagrams of ammonium alum with ammonium- and with aluminum sulfate, exhibiting a sharp eutectic, were fitted by the Ott equation. The magnesium-nitrate-rich part of the diagram with aluminum nitrate is modeled by the BET method.

Keywords: Aluminum salts; BET model; Magnesium salts; Phase diagram; Salt hydrates

1. Introduction

Mixtures of hydrates of inorganic salts may form continuous solid solutions [1,2], eutectics, peritectics, and eventually congruently melting compounds [2,3]. In a project aimed at obtaining thermodynamic properties of salt hydrates that could eventually act as phase change materials for thermal energy storage, the solid–liquid phase diagrams of several such mixtures were studied. Interest was focused on mixtures with melting points between 60 and 100 °C, and four such systems are described here. These are common-ion mixtures, with either a common cation or a common anion. Two of them are based on magnesium nitrate hexahydrate (MgN in the following) that is well-characterized and melts reversibly: its mixtures with magnesium acetate tetrahydrate (MgA) and with aluminum nitrate nonahydrate (AlN). The other two mixtures comprise ammonium alum (AAl) mixed with ammonium sulfate (AS) and with aluminum sulfate hydrate (AlS). The alum is the dodecahydrate, again well-characterized and melting reversibly, but AS is anhydrous and AlS is nominally the octa- or hexadecahydrate. The solid–liquid phase diagrams of these mixtures were studied.

Systems that exhibit a sharp minimum (a eutectic) can be fitted with the semi-empirical Ott equation [4]. For the systems considered in this paper, only the alum-rich part of the $(1-x)$AAl + xAS phase diagram and the entire $(1-x)$AAl + xAlS phase diagram, where x is the mole fraction, can be so fitted with equations:

$$T(x) = T^* \left[1 + \sum a_i (x - x^*)^i\right] \quad (1)$$

In the AAl-rich side $T^* = T_m$(AAl) and $x^* = 1$ with one set of a_i parameters. Since AS was not melted, the AS-rich side of the eutectic at $x_{AS} = 0.6$ could not be fitted. In the second system, in the AAl-rich side $T^* = T_m$(AAl) and $x^* = 1$ with another set of a_i parameters and for the AlS-rich side, beyond the eutectic, $T^* = T_m$(AlS) and $x^* = 0$ with a third set of a_i parameters.

The liquidus of salt hydrates and their mixtures can, in principle, be modeled by the BET method [5,6]. This approach requires data on the vapor pressures of the aqueous salts at their melting point, but of the systems examined here data are available only for MgN. Modeling was, therefore, applied only to the MgN + AlN system. The following expression [5] was first employed to obtain the c and r BET parameters for MgN from the vapor pressures, yielding the water activities, a_W:

$$\frac{m}{55.51}\left[\frac{a_W}{1-a_W}\right] = \frac{1}{cr} + \left[\frac{c-1}{cr}\right] a_W \quad (2)$$

* Corresponding author. Tel.: +972-2-6585341; fax: +972-2-6585319.
E-mail address: ymarcus@vms.huji.ac.il (Y. Marcus).

0040-6031/$ – see front matter © 2003 Elsevier B.V. All rights reserved.
doi:10.1016/j.tca.2003.09.019

where m is the molality of the salt. The parameter r represents the number of binding sites for water in the salt and $c = \exp(\varepsilon/RT)$, where ε represents the difference between the molar enthalpy of "sorption" of water on the salt and the molar enthalpy of liquefaction of water. The activity of the salt is given by the following BET expression [5]:

$$\frac{55.51}{m}\frac{\lambda}{1-\lambda} = \frac{r}{c} + r\left[\frac{c-1}{c}\right]\lambda \tag{3}$$

from which $a_S = \lambda^r$ is obtained. The enthalpy of fusion of MgN, L, and the excess partial molar enthalpies H_S^E and H_W^E, calculated according to the BET expressions [5] yield the quantity $(L - H_S^E - 6H_W^E)/R$, there being six moles of water per mole magnesium in MgN, employed for obtaining the liquidus temperature.

It is assumed [6] that the BET parameters in the MgN + AlN (M and A, for short) mixtures are the mole-fraction-weighted means

$$r = (x_M r_M + x_A r_A) \quad \text{and} \quad \varepsilon = \frac{x_M r_M \varepsilon_M + x_A r_A \varepsilon_A}{r} \tag{4}$$

and $c = \exp(\varepsilon/RT)$, as before. The values of r_A and ε_A for AlN cannot be obtained due to lack of water vapor pressure data at elevated temperatures, so they had to be estimated from room temperature data. The liquidus is then obtained iteratively at various assumed temperatures T for a given composition $x = x_A$ from:

$$\ln[a_S(T,x)a_W^6(T,x)] - \ln[a_S(T_m,1)a_W^6(T_m,1)] = \left\{\frac{L - H_S^E - 6H_W^E}{R}\right\}\left[\frac{1}{T} - \frac{1}{T_m}\right] \tag{5}$$

with T_m being the melting point of MgN, until equality of both sides of Eq. (5) is attained.

2. Experimental

2.1. Materials

AlN: aluminum nitrate nonahydrate (Riedel-DeHaen) ($Al(NO_3)_3{\cdot}9H_2O$) was used as received. Its water content was determined by EDTA (back) titration of the aluminum content and was found to be slightly below 9 mol per mole aluminum. A sample from a new bottle (Fluka) showed slightly more than 9 mol of water per mole salt, determined by weighing after drying in a vacuum oven at 60 °C and 9.18 ± 0.02 mol of water per mole salt, determined by EDTA (back) titration. *AlS*: two batches of aluminum sulfate (Baker' Analyzed) were used: one is nominally $Al_2(SO_4)_3{\cdot}18H_2O$ and the other $Al_2(SO_4)_3{\cdot}16H_2O$, but they actually contained 16.3 ± 0.2 mol water per mole salt, from the water loss on heating to constant weight. They were used as received. *AAl*: ammonium alum (Baker's Analyzed) ($NH_4Al(SO_4)_2{\cdot}12H_2O$) was ground to smaller crystals before being melted. Its water content was determined by EDTA (back) titration of the aluminum content and was found to be 12.10 ± 0.03 mol per mole salt. *AS*: ammonium sulfate (Malinckrodt) ($(NH_4)_2SO_4$) was used as received. *MgN*: magnesium nitrate hexahydrate (Baker's Analyzed) ($Mg(NO_3)_2{\cdot}6H_2O$), water content 6.02 ± 0.01 mol of water per mole salt, determined by EDTA and by Karl–Fischer titrations. *MgA*: magnesium acetate tetrahydrate (Merck) ($Mg(CH_3CO_2)_2{\cdot}4H_2O$) water content 4.00 ± 0.02 mol of water per mole salt, determined by EDTA titration. Several samples of the latter were tested for their water loss in a vacuum oven at 45 °C, and found indeed to lose practically 4.0 mol of water per mole of salt. *Ka*: well-crystallized kaolinite from Washington County, GA, was used as a nucleating agent.

2.2. X-ray characterization

A Philips Automatic Powder Diffractometer was employed, with monochromatized Cu Kα radiation. Crystals of $Al(NO_3)_3{\cdot}9H_2O$ (AlN), $Al_2(SO_4)_3$ (A1S) $16.3H_2O$, $Mg(NO_3)_2{\cdot}6H_2O$ (MgN), and $Mg(CH_3CO_2)_2{\cdot}4H_2O$ (MgA) were ground finely, and their powder diffractions were measured. The diffraction patterns agreed with those in the literature (in the case of AlS with that of nominally $Al_2(SO_4)_3{\cdot}17H_2O$) [2000 JCPDS]. The possibility of a reaction of ammonium alum with kaolinite (Ka), used as the nucleation agent, while the AAl was molten, was examined by keeping 5 and 15 wt.% of Ka in the melt for several hours. After cooling and solidification the samples were ground and subjected to X-ray powder diffraction examination. No lines other than those of pure crystalline AAl and Ka were found.

2.3. Phase diagrams of mixtures

Mixtures of two salt hydrates were prepared on a mole ratio basis, ground lightly together, and samples of approximately 20 g were placed in an open test-tube and melted in an oil bath at ≤10 °C above the melting point. A glass tube with a sealed end having externally little glass bumps, in which a digital thermometer (Ertco-Hart, model 850C) probe was inserted with silicone oil as a heat transfer agent, acted as a manual stirrer. Cooling curves were taken, determined with the digital thermometer, temperatures being read to 0.01 °C every 30 s, stored, and presented graphically in an automatic manner. Generally, the sample tube was freely suspended in air for the melt to cool, but in some cases it was surrounded by insulation in order to slow down the cooling. Some melts refused to crystallize with a halt in the curve without a nucleating agent (then 1% by mass of Ka was added to promote crystallization) but in some cases the melts cooled to a glassy mass. Three cycles of melting–freezing were generally carried out, with results reproducible within ±1 °C. Supercooling of 2–4 °C was found in most cases, but in some the supercooling amounted to 10 °C.

Table 1
Water loss on cycling of salt hydrate mixtures after several melting and solidification cycles

Vessel	Composition	Cycles	Moles water per mole salt			
			Nominal	Before	After	Loss
Open	0.25 AlN + 0.75 MgN	3	6.75	6.80	6.64	0.16
	0.50 AlN + 0.50 MgN	3	7.50	7.40	6.20	1.20
	0.75 AlN + 0.25 MgN	3	8.25	7.95	7.80	0.15
	0.20 MgA + 0.80 MgN	3	5.60	5.51	5.40	0.11
	0.30 MgA + 0.70 MgN	10	5.40	5.36	5.08	0.28
	0.35 MgA + 0.65 MgN	10	5.30	5.20	5.08	0.12
	0.40 MgA + 0.60 MgN	10	5.20	5.18	4.86	0.32
Closed	0.30 MgA + 0.70 MgN	10	5.40	5.36	5.37	−0.01
	0.40 MgA + 0.60 MgN	10	5.20	5.18	5.17	0.01

3. Results

3.1. Stability of the materials on cycling

The water contents of portions of ca. 10 g of certain mixtures of salt hydrates were determined before and after cycling through melting and solidification, in both open and closed vessels. Representative samples of these mixtures were analyzed for their metal ion contents by EDTA titration, from which the water contents were deduced. The results are shown in Table 1. In open vessels the mixtures lost ca. 0.02–0.05 mol of water per mole of salt per cycle. In closed vessels a minimal amount of water condensed on the upper (cooler) walls of the vessel but the overall loss of water was <0.002 mol of water per mole salt per cycle. In mixtures containing magnesium nitrate and acetate the loss of CO_2 by possible oxidation and decomposition of the acetate was checked by elemental analysis after the cycling. The results were inconclusive as regards minor changes, but no major changes in the composition of the salts was detected.

3.2. Individual salts

The melting–freezing points, t_m, are shown in Table 2, together with data from the literature. Molten MgN crystallized readily at $t_m = 89.5 \pm 0.5\,^{\circ}C$. The MgA did not melt readily to a clear liquid and generally showed no breaks in the cooling curves, except in one case, at 46 °C. Pure AlN crystallized at $t_m = 71.0 \pm 0.7\,^{\circ}C$ with ∼8 °C supercooling. However, in other experiments pure AlN on cooling from the melt did not show a break near this temperature, but on the contrary, a clear break was obtained at $47 \pm 3\,^{\circ}C$, with 2–4 °C supercooling. This may signify that water was absorbed, resulting in a higher hydrate with a lower melting point. For pure AAl large supercooling was noted and the following nucleation agents were used. The values of the melting point t_m for 1% soda-lime particles are $91 \pm 1\,^{\circ}C$ (average for four cycles). For 1 and 1.5% powdered silica $t_m = 90 \pm 1\,^{\circ}C$ (average for four samples), for 3 and 4% $t_m = 89 \pm 1\,^{\circ}C$ (average for seven samples). Pure AS, not being a salt hydrate, was not subjected to melting and crystallization. AlS melted at a higher temperature than reported in some of the literature [7,8], 86–88 °C; in fact a much higher temperature, 110 °C, was required to yield a clear liquid (see [10,13], where t_m was shown to depend on the water content). The melt of our sample of AlS then showed a break in the cooling curve at 93.3 °C, taken to be t_m.

3.3. Mixtures of MgN and MgA

The phase diagram is shown in Fig. 1. The main features with increasing MgA content are a maximum near $x_{MgA} = 0.32$, $t_m = 65\,^{\circ}C$, and two minima (eutectics) surrounding it, one near $x_{MgA} = 0.28$, $t_m = 61\,^{\circ}C$, the other near $x_{MgA} = 0.38$, $t_m = 62\,^{\circ}C$. On further increase of the MgA content in the region $0.45 \leq x_{MgA} \leq 0.75$ three cycles of cooling

Table 2
Melting points of salt hydrates

Salt	t_m (°C)	Melting	Reference
AAl	94.5		[8]
	80–94		[9]
	93.8		[7]
11.9-Hydrate	94.0	Congruent	[10]
	93.5	Congruent	[11]
	90 ± 1	Congruent	Present work
AlN	73		[8]
	73.5		[12]
	74.2–76.2		[7]
	70		[9]
	71.0 ± 0.7		Present work
AlS (18-hydrate)	86 dec		[8]
18-Hydrate	88		[7]
17.4-Hydrate	77–108	Gradual	[10]
15.4-Hydrate	90		[13]
16.3-Hydrate	93.3		Present work
MgA	80 dec		[8]
	68		[14]
	67.2		[15]
MgN	∼95 dec		[8]
	89		[7]
	95		[9]
	90.3		[16]
	89.5	Congruent	[17]
	89.5 ± 0.2	Congruent	Present work

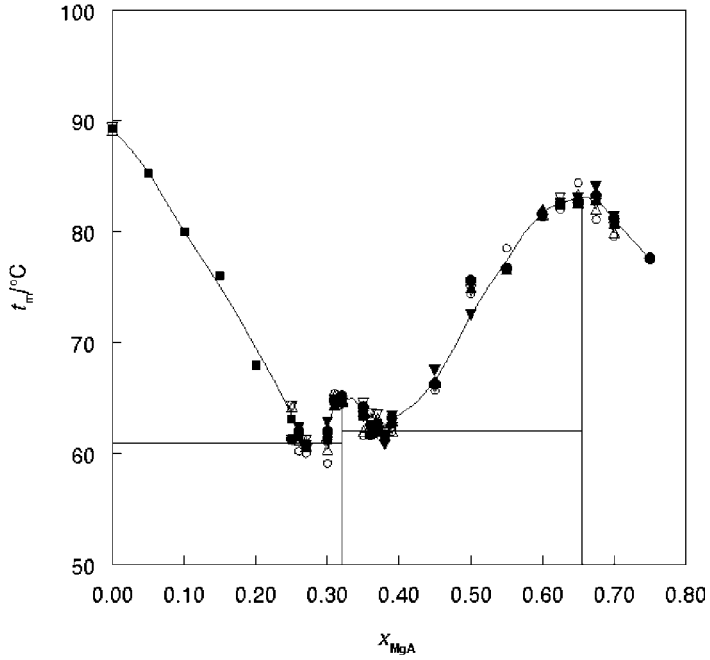

Fig. 1. Phase diagram of MgN+MgA. The freezing point is t_m in °C; (■) first series of experiments, (●) second series of experiments, (○) literature data.

curves were obtained, with and without 1% Ka. Increasing difficulty of crystallization, i.e., no definite halt in the temperature decrease in one of the cycles and solidification to a glassy mass, were noted. The Ka did help somewhat in ensuring crystallization. The main feature of the phase diagram in this region (see Fig. 1) is the apparent formation of a congruently melting ($t_m = 83.0 \pm 0.3$ °C) mixture near $x_{MgA} = 0.65$. Mixtures with more than 80% mole MgA did not crystallize at all (no break in the cooling curve) but formed a glassy solid when sufficiently cooled, even in the presence of Ka. A mixture of MgN + MgA with $x_{MgA} = 0.67$ (mole fraction, 1:2 nitrate to acetate) was melted, crystallized, and some of it was inserted in a vacuum oven overnight at room temperature. A powder diffractogram was taken and some characteristic lines of the original components, but also lines corresponding to a new 1:3 compound (see below) were found. A similar mixture with $x_{MgA} = 0.75$ (1:3 nitrate to acetate) was similarly prepared (melted and crystallized) and its powder diffraction was measured. The diffraction patterns of the un-dried and dried powder samples were measured, and no difference was found. A large proportion of the lines (67%) corresponded to those of the new compound (see below), but characteristic lines of the original components or other phases were also found.

The crystalline double salt that arises in the MgA-rich part of the MgN + MgA phase diagram was characterized by both powder X-ray diffraction and single-crystal diffraction with crystals grown from the melt and for the latter method also from aqueous solutions. The composition $[Mg_2(CH_3CO_2)_3(H_2O)_6]^+NO_3^-$ was confirmed by elemental analysis, X-ray diffraction and Raman spectroscopy as described elsewhere [3].

3.4. Mixtures of MgN and AlN

No nucleating agents were used in a first set of experiments. Supercooling of 2–4 °C was found when ≥40% mole AlN was present, but below this (except for pure MgN) supercooling up to 10 °C was noted. The main features of the phase diagram, Fig. 2, are a shoulder near 40% mole AlN, signifying possible compound formation, and a eutectic at 42 ± 2 °C near 80% mole AlN. Subsequently, mixtures of the two salts with 1% Ka were melted and cooled for three cycles with well-reproducible results. These essentially confirmed the previously obtained results (one to three cycles but without Ka), see Fig. 2.

3.5. Mixtures of AAl and AS

Supercooling of 0.2–4.0 °C was generally found before the halt in the temperature decrease, t_m, signifying crystallization, was noted. The halt temperatures were reproducible to 1 °C. Mixtures with $x_{AS} \geq 0.9$ failed to melt. The resulting phase diagram is shown in Fig. 3, the fitting curve up to $x_{AS} = 0.6$ according to the Ott equation (1) with $T^* = T_m(AAl) = 363$ K and $x^* = 1$. The parameters are shown in Table 3.

A broad minimum in the curve, $t_m \sim 68$ °C, is noted in the range of ca. $0.6 \leq x_{AS} \leq 0.8$. Melts in the range of $0.45 \leq x_{AS} \leq 0.75$ exhibited a second halt in the cooling curve, t_p, also shown in Fig. 3, corresponding to the eutectic in this system. Mixtures up to $x_{AS} = 0.6$ could be cycled through melting and crystallization for a second and third time with t_m reproducible to 2 °C. However, beyond this composition the melts in the second cycle cooled to a glassy

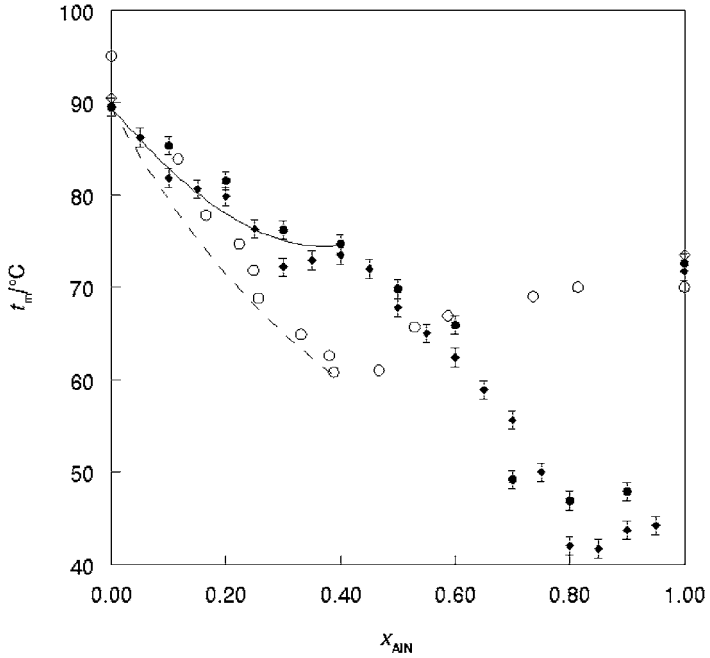

Fig. 2. Phase diagram of MgN + AlN. The freezing point is t_m in °C; (◆) first series of experiments, (●) second series of experiments, (○) literature data from [8] and (◇) from Table 3, (—) BET curve with $\varepsilon = 6.4$ and (– – –) with $\varepsilon = 6.1\,\mathrm{kJ\,mol^{-1}}$.

mass without a significant halt in the temperature. Addition of more Ka, to 5%, did permit crystallization of a mixture with $x_{AS} = 0.65$ in a second cycle, for which the second halt, t_p, was also observed.

The cycling behavior of the AAl+AS mixtures was investigated further for $x_{AS} = 0$, 0.1 and 0.4, ten cycles being followed. In different runs, no additive was used, 1% kaolin was added, or 1 drop of concentrated sulfuric acid was added to 20 g sample (to counteract possible hydrolysis). The results are shown in Table 4. For the first cycle, the values shown in Fig. 3 were found. On subsequent cycles t_m declined slowly for $x_{AS} = 0$ and 0.1, but for $x_{AS} = 0.4$ it first rose considerably for the second cycle and then declined slowly for further cycles. This behavior was observed irrespective of whether

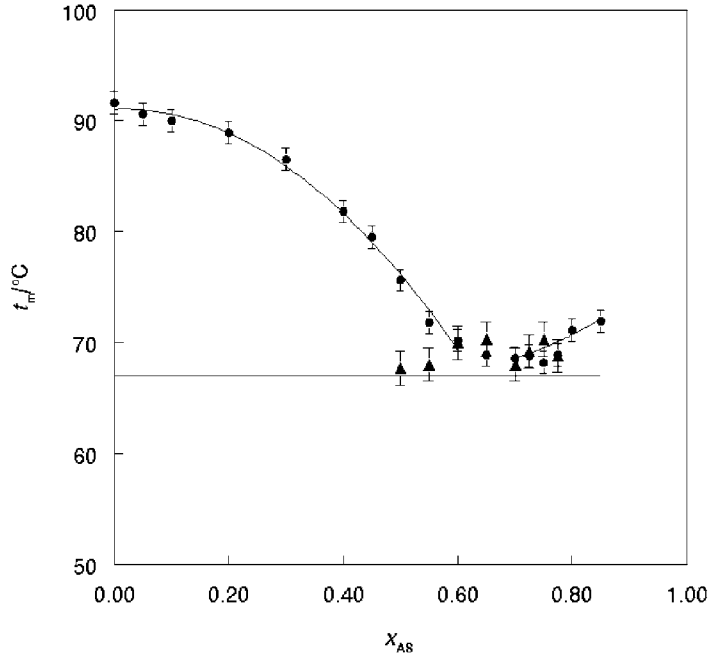

Fig. 3. Phase diagram of AAl + AS. The freezing point is t_m in °C; (●) t_m in series of experiments, (▲) t_p of the eutectic. The curve up to $x_{AS} = 0.6$ was calculated from Eq. (1) with the parameters in Table 3.

Table 3
Parameters of the Ott equation (1) for the alum containing systems

System	x range	T^*	a_0	a_1	a_2
$(1-x)$AAl + xAS	0–0.60	365	−0.171	−0.342	−0.174
$(1-x)$AAl + xAlS	0–0.31	363	−0.394	−0.764	−0.370
$(1-x)$AAl + xAlS	0.31–1.00	367	−0.092	0.187	−0.098

an additive was used or not. The rise in t_m from first to second cycle was also observed for $0.3 \leq x_{AS} \leq 0.6$ (where, except for $x_{AS} = 0.4$, only three cycles were followed). Undercooling of from near 0 up to 8 °C was observed, increasing on increased cycling, again whether an additive was used or not.

3.6. Mixtures of AAl and AlS

This system has a single, well-characterized eutectic at $t_m = 77.0 \pm 1.0$ °C and $x_{AlS} = 0.31 \pm 0.03$. Freezing points were reproducible to ±1 °C in three cycles of melting and freezing. The problem with this system is the uncertainty within ±0.03 of the mole fraction of AlS, due to the uncertainty in its water content. The parameters of the Ott equation (1) with $T^* = T_m(AAl) = 363$ K and $x^* = 1$ for $x_{AlS} \leq 0.31$ and $T^* = T_m(A1S) = 367$ K and $x^* = 0$ for $x_{AlS} \geq 0.31$ are shown in Table 3 and the fitting curves in Fig. 4. On cycling in an open vessel water is lost and the melting point, t_m, increases. Thus, at the eutectic composition, t_m increases up to 84 °C and for $0.75 \leq x_{AlS} \leq 0.95$ t_m values of 96 ± 1 °C were observed.

Table 4
Freezing temperatures on cycling of ammonium alum + ammonium sulfate mixtures, from cooling curves

Cycle no.	Additive	Neat AAl	10% mole AS + AAl	40% mole AS + AAl
1	None	[a]	91.0	80.7
	H_2SO_4	–	91.0	80.5
	1% kaolin	91.4	90.7	81.0
	Average	91.4	90.9	80.7
2–5	None	90.7	88.3	88.8
	H_2SO_4	–	88.8	88.3
	1% kaolin	90.6	90.7[b]	88.3
	Average	90.7	89.3	88.5
6–10	None	87.5[c]	86.4	88.0
	H_2SO_4	–	86.0	87.2
	1% kaolin	92.0[d]	[b]	87.8
	Average	89.8	86.2	87.7

[a] No halt in the cooling curve was observed (cooling too fast?).
[b] Up to 6 cycles only; beyond this a glassy solid resulted on cooling, with no distinct halt in the curve.
[c] Four further cycles were carried out, with average $t_m = 79.3$ °C; over all the n cycles $t_m = 93.5 - 0.78n$ °C.
[d] Cycling only up to the eighth cycle was possible; beyond this a glassy solid resulted on cooling, with no distinct halt in the curve.

4. Discussion

It has been shown by Guion et al. [7] among others, that the melting points of salt hydrates reported in the literature vary considerably. For the salts dealt with in this paper the values are shown in Table 2, including the present t_m values. Our value for AAl is somewhat lower than others', but the supercooling in the present study was considerably reduced, and our value is well-reproducible and appears to be

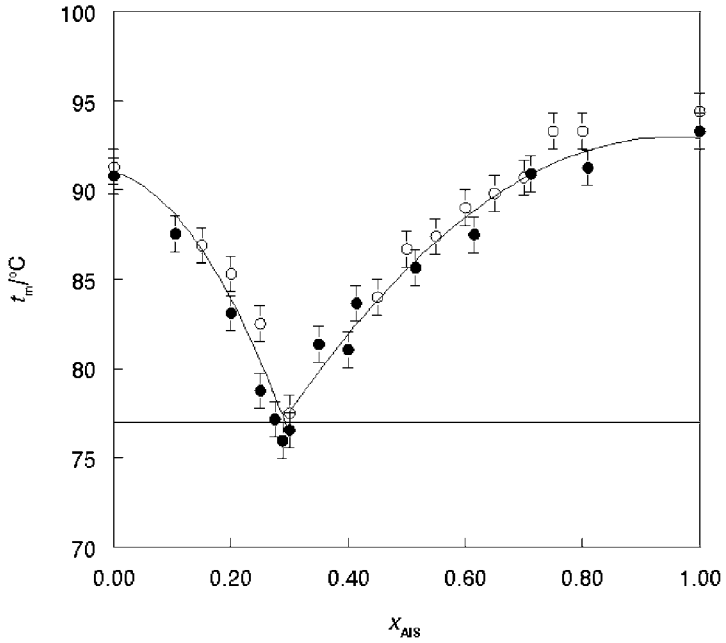

Fig. 4. Phase diagram of AAl + AlS. The freezing point is t_m in °C; (●) first series of experiments, (○) second series of experiments. The curves were calculated from Eq. (1) with the parameters in Table 3.

reliable. MgA could not be melted to a clear melt, and the partly liquefied material (the salt dissolving in its water of crystallization) solidified into a glassy material. The other pure salts had t_m values agreeing with the better characterized literature data.

The only mixture of salt hydrates studied here for which a phase diagram was reported in the literature is MgN + AlN, for which the data by Mokhosoev and Got'manova [9] are shown in Fig. 2. Agreement is poor, in particular as regards the position and the depth of the minimum in the phase diagram. It is noteworthy that these authors reported a much too high melting point for MgN, 95 °C, contrary to the accepted value (Table 2) of 89–90 °C. The water contents in the samples used by Mokhosoev and Got'manova [9] was not specified in the experimental description, only the nominal contents were reported, so the discrepancy may be due to deviating water contents in their sample.

In order to examine the validity of our results for MgN + AlN, an attempt was made to calculate the liquidus for this system by the BET method [5,6]. This could be applied in the MgN-rich part of the phase diagram only, since reliable water vapor pressure data required for the application of the BET method are restricted to aqueous magnesium nitrate at the temperatures involved. According to this method, the activities of water, a_W, and of the salt (here magnesium nitrate), a_S, are calculated at increasing AlN contents at various temperatures to yield the liquidus, T, where pure MgN is at equilibrium with the melt.

Eq. (2) was first employed to obtain the c and r BET parameters for MgN from the vapor pressure data of Mashovets et al. [18] at 90 °C = 363 K = T_m, the melting point of MgN. A least squares evaluation of the left-hand side of Eq. (2) against a_W yielded $r = 4.92$ and $c = 107$. Previous reports of these parameters relate to lower temperatures: at 40 °C $r = 5.70$ and $c = 21.9$ [19] whereas at room temperature $r = 5.58$ and $c = 43.4$ [20]. For molten MgN $m = 55.51/6 = 9.25$ and $a_W = 0.2064$, interpolated in the water activity data [18]. The activity of the salt is given by the BET expression (3), from which $\lambda = 0.0343$ is extricated, hence $a_S = \lambda^r = 6.2 \times 10^{-8}$ is obtained. The alternative derivation of Voigt [20] yields practically the same result: $a_S = 6.6 \times 10^{-8}$. Further required quantities are the enthalpy of fusion of MgN [17,21], $L = 38.5\,\mathrm{kJ\,mol^{-1}}$, and the excess enthalpies $H_S^E = -1.32\,\mathrm{kJ\,mol^{-1}}$ and $H_W^E = 1.50\,\mathrm{kJ\,mol^{-1}}$, calculated according to the BET expressions [5]. The quantity employed is then $(L - H_S^E - 6H_W^E)/R = 3702$ K.

The values of r_A and ε_A for AlN, needed for obtaining the BET parameters in the MgN + AlN mixtures from Eq. (4), cannot be obtained directly, since there are no high temperature water pressure data for aqueous aluminum nitrate that permit the use of Eq. (1). A rough calculation from the activity data of Butsev et al. [22], who reported the Pitzer parameters at 25 °C for up to $m = 3.04\,\mathrm{mol\,kg^{-1}}$, yielded $8 \le r \le 14$ and $6 \le \varepsilon \le 7$. Therefore, assuming these parameters to be independent of temperature, the values $r_A = 11$ and $\varepsilon_A = 6.1$ and $6.4\,\mathrm{kJ\,mol^{-1}}$ were used for further calculations.

The liquidus is then obtained iteratively over a range of temperatures T for a given composition $x = x_A$ from Eq. (5), or, with $T_m = 363$ K

$$\ln[a_S(T,x)a_W^6(T,x)] - \ln[6.2 \times 10^{-8} \times 0.2064^6] = 3702\left[\frac{1}{T} - \frac{1}{363}\right] \quad (6)$$

until equality of both sides of the equation is attained. The resulting (T, x) curves are, however, quite sensitive to the value of ε chosen (much less to that of r), and are shown in Fig. 2 for both values of ε used. It is seen to agree well with the present data for $\varepsilon = 6.4$ but also more or less with the literature ones [9] for $\varepsilon = 6.1$. Thus, the BET modeling, lacking independent values for r_A and c_A, cannot be used to validate either set of experimental liquidus values.

5. Conclusions

The solid–liquid phase diagrams of binary mixtures of salt hydrates are presented. That of magnesium nitrate hexahydrate (MgN, $t_m = 89.5$ °C) with magnesium acetate tetrahydrate (MgA) has a small maximal melting point, 65 °C at a ~2:1 ratio, but a larger one, 83 °C at ~1:2 ratio. However, the substance that crystallizes from the latter melts has the composition $[Mg_2(CH_3CO_2)_3(H_2O)_6]^+NO_3^-$. Mixtures of MgN with aluminum nitrate nonahydrate (AlN, t_m = 70 °C) have a eutectic at 42 °C at a ~1:4 ratio. Mixtures of ammonium alum (AAl, $t_m = 90$ °C) with ammonium sulfate (AS) has a eutectic at 68 °C at a ratio of ~1:3. Mixtures of AAl with aluminum sulfate octa- or hexadecahydrate (AlS, t_m = 93 °C) have a eutectic at 77 °C at a ~2:1 ratio. The latter two phase diagrams, exhibiting a sharp eutectic, were fitted by the Ott equation. The magnesium-nitrate-rich part of the diagram of MgN with AlN was modeled by the BET method. The BET parameters at the melting point of MgN are $c = 107$ and $r = 4.92$, obtained from literature water vapor pressure data on concentrated solutions, but for lack of corresponding data for AlN its parameters had to be estimated. Good modeling was achieved with $c = 9$ and $r = 11$.

Acknowledgements

This research was supported by a grant from the Ministry of Science Culture Sport Israel and Forschungszentrum Juelich GMBH (KFA) within the German-Israeli Energy Research program. Mr. I. Amit is thanked for some of the measurements.

References

[1] Y. Marcus, V. Dangor, S. Lessery, Thermochim. Acta 77 (1984) 216–226.
[2] J.E. Ricci, in: M. Blander (Ed.), Molten Salt Chemistry, Interscience, New York, 1964, pp. 239–253.

[3] Sh. Cohen, L. Ben-Dor, Y. Marcus, J. Cryst. Growth 254 (2003) 151–155.
[4] J.B. Ott, J.R. Goates, J. Chem. Thermodyn. 15 (1983) 267–278.
[5] M.R. Ally, J. Braunstein, Fluid Phase Equil. 87 (1993) 213–236.
[6] M.R. Ally, J. Braunstein, J. Chem. Thermodyn. 30 (1998) 49–58.
[7] J. Guion, D.D. Sauzade, M. Laügt, Therochim. Acta 67 (1983) 167–179.
[8] D.R. Lide (Ed.), Handbook of Chemistry and Physics, 82nd ed., CRC, Boca Raton, 2001–2002.
[9] M.V. Mokhosoev, T.T. Got'manova, Russ. J. Inorg. Chem. 11 (1966) 466–469.
[10] F. Grønvold, K.K. Meisingset, J. Chem. Thermodyn. 14 (1982) 1083–1098.
[11] H.-H. Emons, R. Naumann, K. Köhnke, Z. Anorg. Allgem. Chem. 577 (1989) 83–92.
[12] E. Pietsch, Gmelin Handbook of Inorganic Chemistry, vol. Al 35B, 1934, p. 152, 170.
[13] D. Ornek, T. Gurkan, C. Oztin, Ind. Eng. Chem. Res. 37 (1998) 2687–2690.
[14] A.C.D. Rivett, J. Chem. Soc. (1926) 1064.
[15] K.K. Meisingset, F. Grønvold, J. Chem. Thermodyn. 16 (1984) 523–536.
[16] D. Nikolova, M. Maneva, J. Therm. Anal. 44 (1995) 869–875.
[17] R. Naumann, H.-H. Emons, K. Köhnke, J. Paulik, F. Paulik, J. Therm. Anal. 34 (1988) 1327–1333.
[18] V.P. Mashovets, N.M. Baron, G.E. Zavodnaya, J. Struct. Chem. 7 (1966) 770–773.
[19] S.K. Jain, A.K. Jain, A.K. Gupta, Indian J. Chem. A 24 (1985) 340–342.
[20] W. Voigt, Monatsh. Chem. 124 (1993) 839–848.
[21] Y. Marcus, A. Minevich, L. Ben-Dor, J. Chem. Thermodyn. 35 (2003) 1009–1018.
[22] I.A. Butsev, A.A. Kopyrin, V.V. Proyaev, S.V. Barinov, Soviet Radiochem. 21 (1989) 139–144.